Solid State Sciences 12 (2010) 665–669

Contents lists available at ScienceDirect

Solid State Sciences

journal homepage: www.elsevier.com/locate/ssscie

Ab-initio study of AlN in zinc-blende and rock-salt phases☆

U.P. Verma*,[1], P.S. Bisht

School of Studies in Physics, Jiwaji University, Gwalior – 474011 (M.P.), India

ARTICLE INFO

Article history:
Received 10 August 2008
Received in revised form
12 October 2008
Accepted 9 December 2008
Available online 24 December 2008

Keywords:
Ab-initio calculations
Elastic properties
Transition pressure
Bulk moduli
Phase transition

ABSTRACT

Group III-nitrides are of great interest in both fundamental sciences and technical application. Most of the common nitrides are well known as hard and wide band gap semiconductor materials. In general they have been studied in zinc-blende and wurtzite phases. In this paper, we focus our attention to structural, electronic, phase transition and elastic properties of aluminum nitride (AlN) in zinc-blende and rock-salt phases. A little work has been reported either theoretically or experimentally on elastic and electronic properties of AlN; especially in RS phase. All the calculations are performed using the full-potential linearized augmented plane-wave approach plus local orbitals within the framework of density functional theory as implemented in the Wien2k code. The generalized gradient approximation based on the Perdew–Burke–Ernzerhof is used for the exchange and correlation functional. We determine the full set of first order elastic constants, C_{11}, C_{12} and C_{44} at zero pressure to confirm the mechanical stability and hardness, which have not been established either experimentally or theoretically for RS phase. In the study obvious phase transition from ZB phase to RS phase due to pressure effect has been obtained at 12.75 GPa.

1. Introduction

The III-nitrides are now days widely used by semiconductor industry. Recently there has been increasing scientific and technological interest in wide band gap semiconductors due to several outstanding mechanical properties such as the high melting point, high thermal conductivity, mechanical stability and large bulk moduli. Furthermore, for their electronic properties, in particular for the large band gap and low dielectric constant, the wide band gap semiconductors are promising materials for technological developments of opto- and micro-electronic devices working in the ultra violet spectral region and under high temperature conditions. Among the all group III-nitrides, aluminum nitrides (AlN) have the largest band gap and most of the work reported so far refers to the stable hexagonal wurtzite (WZ) phase of AlN [1,2]. The metastable cubic *zinc-blende* (ZB) modification arises as an advantageous alternative for devices. Despite the technological developments of AlN, few theoretical works are made for ZB [3–6,22] and rock-salt (RS) [7–10] phases.

In this paper, we focus our attention to study structural, electronic, phase transition and elastic properties of AlN in ZB and RS phases employing full-potential linearized augmented plane-wave (FP-LAPW) approach as a little work is reported either theoretically or experimentally on the elastic and electronic properties of AlN in RS phase. The computed results are compared with the previous theoretical calculations and available experimental finding.

2. Computational details

We use the first-principle method to compute total energy for ZB- and RS-AlN under hydrostatic pressure. Hydrostatic pressure is achieved by resizing the volume of the unit cells. The calculations are performed using the FP-LAPW approach plus local orbitals [11,12] within the framework of density functional theory (DFT) [13] as implemented in the Wien2k code [14]. Thus the equilibrium lattice constants of ZB-AlN and RS-AlN compounds are determined by the minimization of the total energy with respect to the volume of the unit cells. Corresponding to minima of the total energy versus unit cell volume, in both the cases, pressure is assumed to be zero.

In the calculations for ZB-AlN we use two atoms per primitive cell, where Al is considered at (0,0,0) and N at (1/4,1/4,1/4) positions. In the case of RS-AlN two atoms per primitive cell are also

☆ This paper was presented at the "Second International Symposium on Structure–Property Relationship in Solid State Materials" (Nantes, France; June 29-July 03, 2008).

* Corresponding author. Tel.: +91 751 2442782.
E-mail address: upv.udai@gmail.com (U.P. Verma).
[1] Present address: FB C – Mathematik und Naturwissenschaften, Bergische Universitaet, Wuppertal – 42119, Germany.

1293-2558/$ – see front matter © 2008 Elsevier Masson SAS. All rights reserved.
doi:10.1016/j.solidstatesciences.2008.12.002

taken but considering Al at (0,0,0) and N at (1/2,1/2,1/2) positions. In order to decide optimum number of k-points plots between total energy and number of k-points were drawn. On the basis of the convergence of the total energy we use 1000 k-points for the ZB structure and 1200 k-points for the RS structure within Brillion zone. The k-points' sets used in the calculations are based on a $10 \times 10 \times 10$ divisions of the reciprocal unit cells that results into 45 equivalent k-points due to symmetry, in both types of AlN.

To begin FP-LAPW computation the unit cell is partitioned into non-overlapping muffin-tin spheres around the atomic sites, and an interstitial region. Inside the atomic spheres, the basis set used to describe electronic states employ atomic like function, while in the interstitial region plane waves are used. The exchange–correlation potential is calculated by generalized gradient approximation (GGA) based on the Perdew–Burke–Ernzerhof (PBE) approach [15]. In the ZB-AlN structure the muffin-tin (MT) sphere radii of 1.72 and 1.62 Bohr are used for Al and N atoms, respectively, while in the RS-AlN structure corresponding MT sphere radii of 1.70 and 1.60 Bohr are used because the lattice constants of the two structures are different. The valence wave functions inside the MT sphere are expended into spherical harmonics up to $l = 10$ and the $R_{mt}K_{max}$ are taken to be 7.0. Also, the self-consistent calculations stop only when the total energy and the charge of the system meet the convergence limit of 0.0001 eV and 0.001 eV, respectively. This method has been proved successful in the determination of the structural and mechanical properties of the semiconductor materials [16].

3. Results and discussion

3.1. Structural properties

In this study, the exchange–correlation potential functional, under GGA approach, are employed to characterize the atomic behavior in cubic phase ZB- and RS-AlN under ambient condition. Fig. 1 shows the calculated energy–volume curves for ZB and RS-AlN. In both the cases seven points were calculated. The calculated values of lattice constants along with their experimental and earlier reported values are listed in Table 1. In comparison with the experimental values, error in the lattice constant of ZB-AlN is ~2.28% and that in RS-AlN is ~0.5%. Also errors in the calculation of equilibrium bulk modulus in comparison with the experimental values are ~3.21% and 13.78%, respectively, for ZB-AlN and RS-AlN. The amount of error shows that the reported results are acceptable and hence other predictions can be forecasted on the basis of computational results.

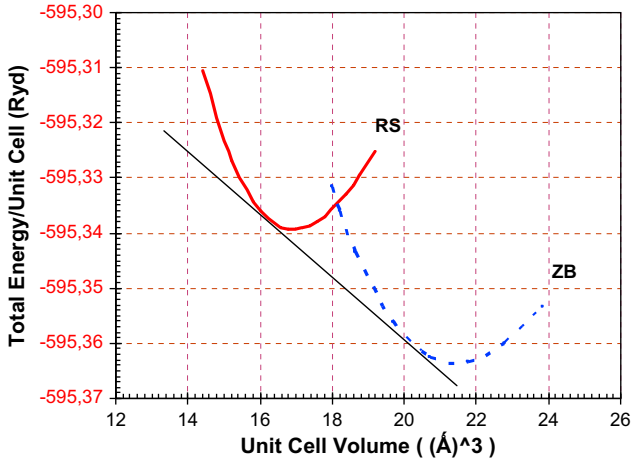

Fig. 1. Plot of total energy per unit cell (in Ryd) as a function of unit cell volume (in Å^3) for AlN in ZB and RS structures.

Table 1
Calculated theoretical equilibrium lattice constant, bulk modulus and transition pressure of ZB and RS-AlN using Murnaghan equation of state [17].

AlN phase	Lattice constant		Bulk moduli B		Transition pressure(ZB → RS)	
	a (in Å)	Reference	(in GPa)	Reference	P_t (in GPa)	Reference
ZB	4.38	PW	195.5	PW	12.75	PW
	4.37	[18]^E	202	[20]^E	7.1	[6]
	4.302	[10]	194.028	[8]	12.9	[25]
	4.377	[8]	203.2	[21]	14–16.6	[18]
	4.379	[6]	209	[10]	14–20	[24]
			216	[22]	16.6	[4,22]
			224	[6]		
RS	4.07	PW	254.3	PW		
	4.05	[19]^E	295	[23]^E		
	4.03	[8]	221	[24]		
	3.978	[10]	272	[10]		
	4.23	[6]	270	[22]		
	3.982	[7]	256.89	[8]		
			297.6	[6]		
			329	[7]		

PW = Present work.
E = Experimental.

From figure it is clear that the total energy per formula unit of the ZB phase is about 0.021 Ryd smaller than that of the RS phase. This indicates that the zero pressure may be taken corresponding to the minima of ZB-AlN. At a sufficient high pressure the RS phase is favored. The transition pressure is the pressure at which enthalpy ($H = E + PV$) of the ZB-AlN phase equals to that of the RS-AlN phase. The common tangent gradient gives equilibrium transition pressure (P_t) at 12.75 GPa. The maximum amount of error in the calculation of transition pressure is ~14%. The value of transition pressure is in good agreement with earlier reported transition pressure by others [4,18,22,24,25].

The curves in Fig. 1 are obtained by calculating the total energy at seven different volumes around equilibrium of AlN in ZB as well as in RS phases and by fitting the calculated values to the Murnaghan equation of state [17].

$$E_T(V) = E_0 + \frac{B_0 V}{B_0'}\left[\frac{(V_0/V)^{B_0'}}{B_0' - 1} + 1\right] - \frac{V_0 B_0}{B_0' - 1} \tag{1}$$

In this equation V_o is the value of unit cell volume V, B_0 is the bulk modulus, B and B_0' is pressure derivative of the bulk modulus corresponding to the minima of the total energy versus unit cell volume curve. The bulk modulus B, its derivative B' and pressure corresponding to various values of volume are calculated using following relations:

$$B = V\frac{d^2E_T}{dV^2} \tag{2}$$

$$B' = \left(\frac{\partial B}{\partial P}\right)_T \tag{3}$$

and

$$P(V) = \frac{B_0}{B_0'}\left[\left(\frac{V_0}{V}\right)^{B_0'} - 1\right] \tag{4}$$

From the Murnaghan fit of the total energy versus unit cell volume the bulk modulus, B, and the equilibrium lattice constants, a, of AlN in ZB and RS phases are determined. The calculated values of bulk modulus are in good agreement with other experimental and theoretical works as listed in Table 1. From Table 1 it is observed that bulk modulus of RS-AlN is higher than ZB-AlN. It implies that

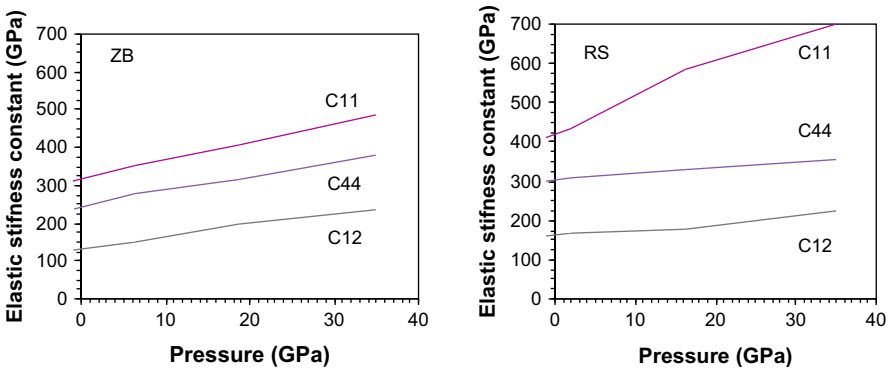

Fig. 2. Plot of elastic moduli (in GPa) as a function of pressure (in GPa) for ZB- and RS-AlN.

the AlN in RS phase is mechanically more stable than ZB phase. Our calculated transition pressure and lattice constants are also in good agreement with earlier reported theoretical works, included in Table 1.

3.2. Elastic properties

In this section we investigate the high-pressure behavior of the elastic moduli for cubic AlN. Elastic constants are one of the important technological properties of solids. They determine the behavior of materials under sufficient small loading because of the fact that the elasticity of simple crystals is a local property.

A cubic system possesses three independent lattice constants C_{11}, C_{12} and C_{44}. The condition for elastic stability is that under hydrostatic pressure [26], $C_{11}+C_{12}>0$, $C_{44}>0$ and $C_{11}-C_{12}>0$. These conditions are called mechanical stability criteria. The first term in the mechanical stability criteria is closely related to the bulk modulus, which is obviously necessary for stability. The later two terms of the mechanical stability are thought to play a more subtle role since C_{44} involves shearing of the Al–N bonds and $(C_{11}-C_{12})$ involves stretching (and compression) of the Al–N bonds with a combination of bending and starching of Al–Al bonds.

The elastic stiffness constants are obtained by fitting the total energy of the strained crystal to polynomial of the strains (Eq. (1)). Since there are three independent elastic constants for a cubic phase, three types of strains, viz, volume conserved monoclinic strain, tetragonal shear strain and rhombohedral shear strain may be applied to the optimized structures to calculate the elastic constants.

For calculating C_{11} and C_{12} the tetragonal strain transforms the lattice vector as [27,28]

$$R' = \varepsilon R \tag{5}$$

Here $\acute{R}$ and R are the new and old lattice vectors, respectively and ϵ is the strain tensor expressed in terms of the tetragonal shear deformation parameter δ as:

Table 2
Calculated theoretical equilibrium elastic constant of ZB- and RS-AlN.

AlN Phase	Elastic constants (in GPa)			Anisotropy parameter	Ref.
	C_{11}	C_{12}	C_{44}	A	
ZB	315	130	245	2.64	PW
	330.71	162.199	156.41	1.85	[8]
	310.4	180	96	1.47	[10]
	294–313	152–168	78–202	1.25–2.84	[3]
RS	420	165	300	2.35	PW

$$\overleftrightarrow{\varepsilon}_{\text{tetra}} = \begin{pmatrix} 1+\delta & 0 & 0 \\ 0 & 1-\delta & 0 \\ 0 & 0 & 1/(1-\delta^2) \end{pmatrix} \tag{6}$$

Application of this tensor modifies the total energy from its unstrained value to the strained one. In the case of cubic lattice it is possible to choose stain so that the volume of the unit cell is preserved as well as the energy be the function of the even power of the strain constant. Thus total energy can be expressed as a function of δ as [29,30]

$$E(\delta) = E(-\delta) = E_0 + (C_{11}-C_{12})^*V^*\delta^2 + O(\delta^4) \tag{7}$$

Here V is the volume of the unit cell and E_0 is the energy of the unstrained lattice at volume V. For isotropic cubic crystal, the following relation gives the bulk modulus, B, as

$$B = \frac{1}{3}(C_{11}+2C_{12}) \tag{8}$$

Equations (7) and (8) provide direct information about C_{11} and C_{12} parameters.

Further the volume conserving monoclinic strain tensor is given as [20]

$$\overleftrightarrow{\varepsilon}_{\text{monoclinic}} = \begin{pmatrix} 1 & \delta'/2 & 0 \\ \delta'/2 & 1 & 0 \\ 0 & 0 & 4/(4-\delta'^2) \end{pmatrix} \tag{9}$$

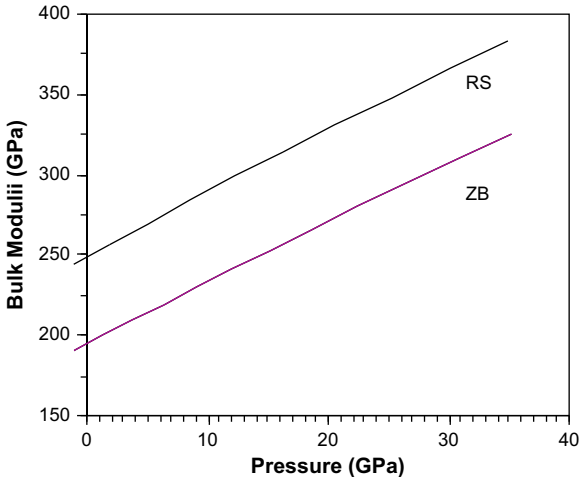

Fig. 3. Plot of bulk moduli B (in GPa) as a function of pressure (in GPa) for ZB- and RS-AlN.

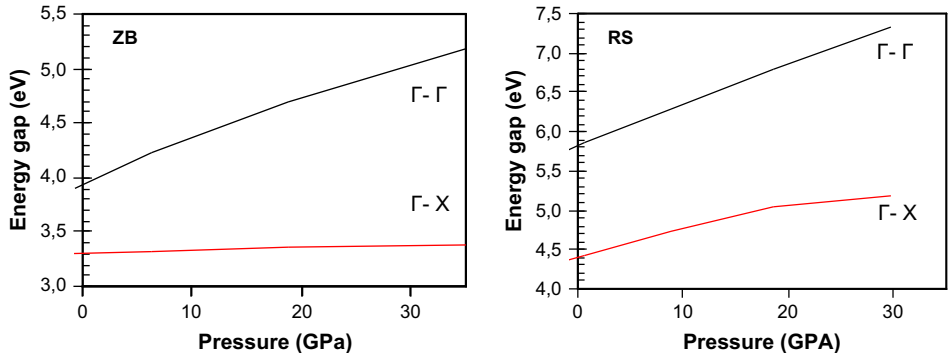

Fig. 4. Plots of (Γ–Γ) and (Γ–X) energy band gaps (in eV) as a function of pressure (in GPa) for ZB- and RS-AlN.

where δ' is the distortion due to change in total energy of the unit cell volume. It can be applied to calculate C_{44} through the expression

$$E(\delta') = E(-\delta') = E_0 + \frac{1}{2}C_{44}{}^{*}V^{*}\delta'^2 + O(\delta'^4) \quad (10)$$

In this equation also the strain energy is having only even order terms of distortion δ'.

The elastic anisotropy of a cubic crystal can be characterized by the Zener anisotropy ratio A, which represents the ratio of the two elastic–shear coefficients [31]

$$A = 2^{*}C_{44}/(C_{11} - C_{12}) \quad (11)$$

For isotropic media $A = 1$.

The calculated elastic stiffness constants C_{11}, C_{12}, C_{44} for ZB-AlN and RS-AlN are shown in Fig. 2. The plots in it show the pressure dependence of the elastic constants. All the constants increase monotonically with the increase in pressure. From Fig. 2 it is also observed that the inequality $C_{11} > C_{44} > C_{12}$ in both the phases of AlN are satisfied over the shown range of the pressure and their values for RS-AlN are higher than that of ZB-AlN.

The Zener anisotropy ratio 'A' based on our present reported elastic constants has been obtained for ZB-AlN and RS-AlN, respectively, 2.64 and 2.35. These values of 'A' show that AlN possesses elastic anisotropy. Table 2 comprises the calculated elastic constants at zero pressure along with Zener anisotropy ratio A. We also calculated the Zener anisotropy ratio corresponding to earlier reported data and included in Table 2. Our calculated values of C_{11} are in excellent agreement with earlier reported data. The values of C_{12} are also in good agreement but our calculated values of C_{44} are more than the earlier reported data. As and when experimental results will be available, justification about validity of the reported data can be tested. The same is true with RS-AlN. For RS-AlN, so far as we know, this information is reported for the first time.

Aggregate values of the bulk modulus, B, with respect to various pressures are shown in Fig. 3. The bulk modulus increases with the increase in pressure and reaches 300 and 375 Gpa, respectively, for ZB and RS-AlN at a pressure of 35 Gpa. For this wide range of pressure the calculated bulk moduli for RS-AlN is greater than the bulk moduli of ZB-AlN.

From Fig. 3 it is interesting to note that at 28 Gpa of pressure the bulk modulus of RS-AlN reaches to 348 Gpa which corresponds to the bulk modulus of the superconducting phase of NbN [32]. At 30 Gpa of pressure the bulk modulus of RS-AlN (369 GPa) corresponds to the the zero pressure value of the bulk modulus of cubic BN [33]. It is known that BN is harder than NbN, therefore, behavior of the bulk moduli (Fig. 3) suggests an increasing hardness in the ZB- and RS-AlN with the increase in pressure.

3.3. Electronic properties

Fig. 4 shows plots of (Γ–X) energy band gaps versus pressure in the ZB- and RS-AlN. The calculated optical band gaps (Γ–X) at zero pressure are 3.31 and 4.40 eV for ZB- and RS-AlN, respectively. Both the structures are indirect band gap materials and their values increase monotonically with increase in pressure. Moreover, the (Γ–Γ) energy band gaps against pressure are also plotted in the same figure. The (Γ–Γ) energy band gap also increases monotonically with increase in pressure. The obtained indirect band gap for ZB-AlN, 3.31 eV is somewhat lower than the experimental reported values, 5.4 eV [34] but in good agreement with the earlier reported theoretical band gaps 3.1 eV [35] and 3.24 eV [8]. Corresponding to the same pressure ZB-AlN possesses lower value of band gap than that of RS-AlN. Our calculated value of energy band gap in the case of RS-AlN, 4.40 eV is in close agreement with recently reported value 4.53 eV [36]. However RS phase is lacking such data experimentally.

4. Conclusions

We present a detailed study of electronic and structural properties of ZB- and RS-AlN. With the increase in pressure a phase transition from ZB-AlN to RS-AlN occurs at 12.75 GPa of pressure. In the fit of total energy versus volume of the unit cell, the minimum of the ZB-AlN is lower than that of RS-AlN. This implies that basic structure wise ZB-AlN is more stable than RS-AlN. When strain is applied on both phase materials, we find that RS-AlN is more rigid than ZB-AlN. Thus we conclude that AlN in RS phase has high intrinsic strength, therefore, it may be used as an anti-oxidant agent for protection from oxidation.

Acknowledgements

One of the authors (UPV) would like to thank Prof. Per Jensen for fruitful discussions and sincere cooperation extended by him during his stay at Wuppertal. Financial support from Alexander von Humboldt Foundation to (UPV) is gratefully acknowledged. Discussions held with Dr. U.S. Sharma are also thankfully acknowledged.

Appendix. Supporting information

Supplementary data associated with this article can be found, in the online version, at doi:10.1016/j.solidstatesciences.2008.12.002

References

[1] S.C. Jain, M. Willander, J. Narayan, R. van Overstraeten, J. Appl. Phys. 87 (2000) 965.
[2] A.G. Bhuiyan, A. Hashimoto, A. Yamamoto, J. Appl. Phys. 94 (2003) 2779.
[3] K. Kim, W.R. L Lambrecht, B. Segall, Phys. Rev. B 53 (1994) 310.

[4] N.E. Christensen, I. Gorczyca, Phys. Rev. B 50 (1994) 4397.
[5] K. Karch, J.M. Wagner, F. Bechstedt, Phys. Rev. B 57 (1998) 7043;
A.F. Wright, J. Appl. Phys. 82 (1997) 2833.
[6] S. Goumri-Said, M.B. Kanoun, A.E. Merad, G. Merad, H. Aourag, Chem. Phys. 302 (2004) 135.
[7] Ravindra Pandey, Amin Sutjianto, Max Seel, John E Jaffe, J. Mater. Res. 8 (1993) 1922.
[8] Y.Ö. Ciftci, K. Colakoğlu, E. Deligöz, Phys. Status. Solidi. C 4 (2007) 234–237.
[9] C.C. Silva, H.W. Leite Alves, L.M.R. Scolfaro, J.R. Leite, Phys. Status. Solidi. C 2 (7) (2005) 2468.
[10] Jorge Serrano, Angel Rubio, E. Hernandez, A. Munoz, Phys. Rev. B 62 (2000) 16612.
[11] E. Sjostedt, L. Nordstrom, D.J. Singh, Solid State Commun. 114 (2000) 15.
[12] G.K.H. Madsen, P. Blaha, K. Schwarz, E. Sjostedt, L. Nordstrom, Phys. Rev. B 64 (2001) 195134.
[13] P. Hohenberg, W. Kohn, Phys. Rev. 136 (1964) 864.
[14] P. Blaha, K. Schwarz, P.I. Sorantin, S.B. Trickey, Comput. Phys. Commun. 59 (1990) 399;
K. Schwarz, P. Blaha, G.K.H. Madsen, Comput. Phys. Commun. 147 (2002) 71;
K. Schwarz, P. Blaha, Comput. Mater. Sci. 28 (2003) 259.
[15] J.P. Perdew, S. Burke, M. Ernzerhof, Phys. Rev. Lett. 77 (1996) 3865.
[16] F. Litimein, B. Bouhafs, Z. Dridi, P. Ruterana, New J. Phys 4 (2002) 64.
[17] F.D. Murnaghan, Proc. Natl. Acad. Sci. U.S.A. 30 (1994) 5390.
[18] C. Stampfl, C.G. Van de Walle, Phys. Rev. B 59 (1999) 5521.
[19] H. Vollstädt, E. Ito, M. Akaishi, S. Akimoto, O. Fukunaga, Proc. Jpn. Acad. Ser. B: Phys. Biol. Sci. 66 (1990) 7.
[20] M.E. Sherwin, T.J. Drummond, J. Appl. Phys. 69 (1991) 8423.
[21] S.Q. Wang, H.Q. Ye, J. Phys. Condens. Matter 14 (2002) 9579.
[22] N.E. Christensen, I. Gorczyca, Phys. Rev. B 47 (1993) 4307.
[23] S. Uehara, T. Masamoto, A. Onodera, M. Ueno, O. Shimomura, K. Takemura, J. Phys. Chem. Solid. 58 (1997) 2093.
[24] Q. Xia, H. Xia, A.L. Ruoff, J. Appl. Phys. 73 (1993) 8198.
[25] P.E. Van Camp, V.E. Van Doren, J.T. Devreese, Phys. Rev. B. 44 (1991) 9056.
[26] J.F. Nye, Physical Properties of Crystal, Oxford Univ. Press, 1985.
[27] M. Dacorogna, J. Ashkenazi, M. Peter, Phys. Rev. B 26 (1982) 1527.
[28] N.E. Christensen, Solid State Commun. 49 (1984) 701.
[29] M.J. Mehl, Phys. Rev. B 47 (1993) 2493.
[30] R. Khenata, A. Bouhemadou, Ali H Reshak, R. Ahmed, B. Bouhafs, D. Rached, Y. Al-Douri, M. Rerat, Phys. Rev. B 75 (2007) 195131.
[31] H. Ledbetter, A. Miglioria, J. Appl. Phys. 100 (2006) 063516.
[32] Xiao-Jia Chen, Viktor V Struzhkin, Zhigang Wu, Ronald E. Cohan, Russel J. Hemley, PNAS 102 (2005) 9.
[33] C. Lee, W. Yang, R.G. Parr, Phys. Rev. B 37 (1988) 785.
[34] I. Vurgaftman, J.R. Meyer, L.R. Ram-Mohan, J. Appl. Phys. 89 (2001) 518;
I. Vurgaftman, J.R. Meyer, J. Appl. Phys. 94 (2003) 3675.
[35] P. Jonnard, N. Capron, F. Semond, J. Massies, E. Martinez-Guerrero, H. Mariette, Eur. Phys. J. B 42 (2004) 351.
[36] X. Zhang, Z. Chen, S. Zhang, R. Liu, H. Zong, Q. Jing, G. Li, M. Ma, W. Wang, J. Phys. Condens. Matter 19 (2007) 425231.